G-Quadruplex Stabilizer 3,6-Bis(1-Methyl-4-Vinylpyridinium)Carbazole Diiodide Induces Accelerated Senescence and Inhibits Tumorigenic Properties in Cancer Cells

Fong-Chun Huang,[1] Cheng-Chung Chang,[2] Pei-Jen Lou,[3] I-Chun Kuo,[2] Chih-Wei Chien,[2] Chin-Tin Chen,[4] Fu-Ying Shieh,[1] Ta-Chau Chang,[2] and Jing-Jer Lin[1]

[1]Institute of Biopharmaceutical Sciences, National Yang-Ming University; [2]Institute of Atomic and Molecular Sciences, Academia Sinica; [3]Department of Otolaryngology, National Taiwan University Hospital; [4]Center for Optoelectronic Biomedicine, College of Medicine, National Taiwan University, Taipei, Taiwan, Republic of China

Abstract

Carbazole derivatives that stabilized G-quadruplex DNA structure formed by human telomeric sequence have been designed and synthesized. Among them, 3,6-bis(1-methyl-4-vinylpyridinium)carbazole diiodide (BMVC) showed an increase in G-quadruplex melting temperature by 13°C and has a potent inhibitory effect on telomerase activity. Treatment of H1299 cancer cells with 0.5 μmol/L BMVC did not cause acute toxicity and affect DNA replication; however, the BMVC-treated cells ceased to divide after a lag period. Hallmarks of senescence, including morphologic changes, detection of senescence-associated β-galactosidase activity, and decreased bromodeoxyuridine incorporation, were detected in BMVC-treated cancer cells. The BMVC-induced senescence phenotype is accompanied by progressive telomere shortening and detection of the DNA damage foci, indicating that BMVC caused telomere uncapping after long-term treatments. Unlike other telomerase inhibitors, the BMVC-treated cancer cells showed a fast telomere shortening rate and a lag period of growth before entering senescence. Interestingly, BMVC also suppressed the tumor-related properties of cancer cells, including cell migration, colony-forming ability, and anchorage-independent growth, indicating that the cellular effects of BMVC were not limited to telomeres. Consistent with the observations from cellular experiments, the tumorigenic potential of cancer cells was also reduced in mouse xenografts after BMVC treatments. Thus, BMVC repressed tumor progression through both telomere-dependent and telomere-independent pathways. (Mol Cancer Res 2008;6(6):955–64)

Received 6/6/07; revised 1/7/08; accepted 2/27/08.
Grant support: Academia Sinica grant 5202401023, National Science Council grants 94-2311-B-010-012 and 94-3112-B-010-020, and National Health Research Institute grant NHRI-EX95-9436SI.
The costs of publication of this article were defrayed in part by the payment of page charges. This article must therefore be hereby marked *advertisement* in accordance with 18 U.S.C. Section 1734 solely to indicate this fact.
Note: F-C. Huang and C-C. Chang contributed equally to this work.
Requests for reprints: Jing-Jer Lin, Institute of Biopharmaceutical Science, National Yang-Ming University, Taipei 11221, Taiwan, Republic of China. Phone: 886-2-28267258. E-mail: jjlin@ym.edu.tw or Ta-Chau Chang, Institute of Atomic and Molecular Sciences, Academia Sinica, P. O. Box 23-166, Taipei 106, Taiwan, Republic of China. E-mail: tcchang@po.iams.sinica.edu.tw

doi:10.1158/1541-7786.MCR-07-0260

Introduction

Normal human somatic cells have limited proliferative capacities termed replicative senescence. It is well accepted that telomere shortening on every cell division is one of the possible causes of senescence (1). Telomeres play a vital role in protecting the ends of chromosomes and preventing chromosomal fusion (2, 3). Telomeres of human chromosomes consist of 5 to 15 kbp of TTAGGG repeats that terminate with around 50 to 300 bases of TTAGGG single-strand overhang. Telomerase is a ribonucleoprotein that is involved in telomere replication (4). It used its RNA component as the template to extend telomeric DNA sequences. Telomerase is detected in around 85% to 90% of tumor and cancer cells, whereas it is only expressed at very low level or nondetectable in most somatic cells (5). Because telomere maintenance is required for unlimited proliferation of cancer cells, and owing to its selective presence in most cancer cells, it has been the target for the development of anticancer agents (6).

Several approaches have been developed to identify telomerase inhibitors (7). For example, oligonucleotides targeting the template region of telomerase RNA were shown to be very effective in inhibiting telomerase activity and limiting cancer cell growth (8). Small molecular weight compounds were also identified for telomerase inhibition (9). However, because the telomere shortening rate is around 50 to 200 bp for every cell division (10, 11), inhibiting telomerase would still need to take a long time for telomeres in cancer cells to be shortened to critical length (8). Thus, it was proposed that telomerase inhibition should be accompanied by other anticancer treatments to achieve its best anticancer effects (7). Indeed, a telomerase inhibitor was shown to sensitize the effectiveness of conventional anticancer chemotherapeutics or a tyrosine kinase inhibitor, imatinib (12-15).

The G-rich single-strand tail of telomere could base pair with each other to adopt an intramolecular G-quadruplex structure (16). Because the G-quadruplex DNA structure formed by telomeric DNA is not a substrate of telomerase (17), molecules that stabilize G-quadruplexes have the potential to interfere

with telomere replication by blocking the substrate accessibility of telomerase. It was suggested that quadruplex stabilizers could serve as antitumor agents (18, 19). For example, G-quadruplex stabilizers, such as phenanthrolines triazines, have been shown to act as potent telomerase inhibitors (20-24).

We have recently designed and synthesized a series of carbazole derivatives; among them, 3,6-bis(1-methyl-4-vinylpyridinium)carbazole diiodide (BMVC) was shown to bound to G-quadruplex DNA formed by human telomeric DNA sequences and inhibit telomerase activity (Fig. 1A; refs. 25, 26). Here, we analyze the cellular effects of this compound. We found that BMVC induced an accelerated senescence phenotype in H1299 cancer cells. To our surprise, the cell migration, colony-forming ability, and anchorage-independent growth of BMVC-treated cancer cells were greatly reduced and the *in vivo* tumorigenic properties of cancer cells were decreased with BMVC treatments. These results indicated that BMVCs have multiple inhibitory effects on cancer cells. The property of BMVC supports it as a potential candidate to be developed as an antitumor agent.

Results

BMVC Is a Potent G-Quadruplex Stabilizer and Telomerase Inhibitor

We have previously identified a carbazole derivative, BMVC, as a potent G-quadruplex stabilizer and telomerase inhibitor (25, 26). BMVC has cationic charge on the two pendant groups of pyridinium rings of carbazole (Fig. 1A). To evaluate the effect of BMVC to the G-quadruplex DNA of human telomeric sequences, $d(T_2AG_3)_4$ (Hum), we applied circular dichroism to monitor the melting temperature (*Tm*) of Hum quadruplexes. It has been documented that parallel four-stranded quadruplexes give a positive band ~260 nm and a negative band ~240 nm (27), whereas antiparallel folded quadruplexes have two positive bands around 245 and 290 nm and a negative band ~265 nm (28). The 295-nm circular dichroism band was measured as a function of temperature to determine the *Tm* of Hum24 quadruplexes in the presence of carbazole and BMVC (29). We found that the *Tm* of Hum quadruplexes could be increased more than 10°C on interaction with BMVC, suggesting that it could thermally stabilize the Hum quadruplexes (Fig. 1B). Because the formation of G-quadruplex blocks telomerase extension, the effects of G-quadruplex stabilizer on telomerase activity were analyzed.

A modified telomerase assay, telomeric repeat amplification protocol (TRAP-G4), was used to evaluate the effects of carbazole derivatives on G-quadruplex for inhibiting telomerase activity (30). In the TRAP-G4 assay, a G-quadruplex sequence was introduced into the telomerase extension primer that is susceptible to form an intramolecular G-quadruplex. Figure 1C (*left*) shows the TRAP-G4 assays of the carbazole and BMVC. The telomerase IC_{50} values were estimated to be >10 μmol/L for carbazole and ~0.2 μmol/L for BMVC. The direct inhibitory effect of telomerase was also evaluated by conventional TRAP assays (31). Our results indicated that BMVC has an IC_{50} values against at ~0.2 μmol/L (Fig. 1C, *right*). In both assays, an internal control was included to evaluate the effects of inhibitors toward Taq DNA polymerase (Fig. 1C, *IC*). Our results indicated that BMVC did not affect the Taq DNA polymerase activity in the concentration ranges we tested here (Fig. 1C). To further rule out the possible inhibitory effects of PCRs caused by G-quadruplex stabilizers (32), BMVC was added after the telomerase extension step of the TRAP assays (Fig. 1D). A complete inhibition of the assay was observed at

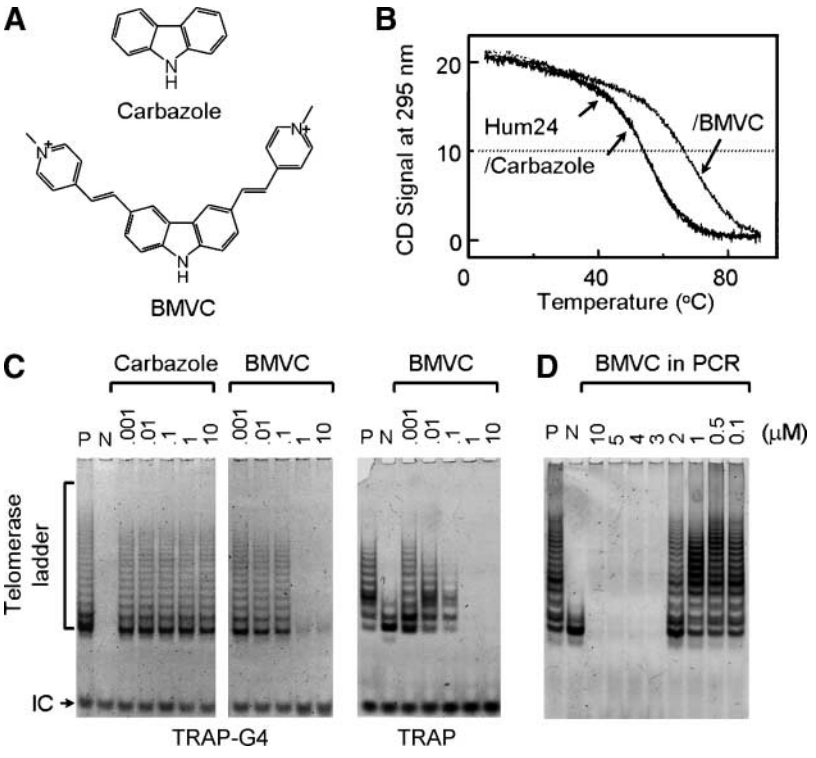

FIGURE 1. Structure and isolation of G-quadruplex stabilizing carbazoles. **A.** Structure of carbazole and BMVC. **B.** BMVC enhances the *Tm* of Hum quadruplex. Temperature-dependent circular dichroism (*CD*) signals at 295 nm of quadruplex $d(T_2AG_3)_4$ (*Hum24*) and on interaction with carbazole and BMVC were measured, respectively. **C.** BMVC inhibits telomerase activity. The effects of BMVC on telomerase activity were measured using TRAP-G4 (*left*) or standard TRAP (*right*) assays (see Materials and Methods). In standard TRAP assays, various amounts of BMVC were incubated with telomerase-active cell extracts for 5 min at room temperature before the telomerase extension reactions. Telomerase-active cell extracts were prepared from H1299 cells (*P*). RNase A–treated extracts were used as negative controls (*N*). The positions of telomerase ladders and internal controls (*IC*) are indicated. **D.** The effects of BMVC on PCRs. The inhibitory effects of BMVC on Taq polymerase were determined in TRAP assays. Indicated amounts of BMVC were added to the TRAP reactions after the telomerase extension steps. PCRs were then conducted as in standard TRAP assays.

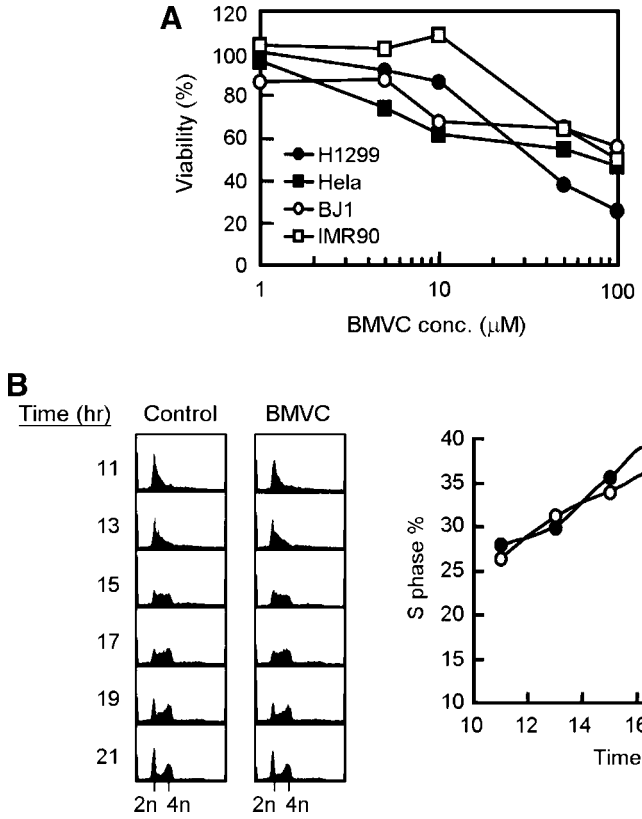

FIGURE 2. BMVC does not cause acute cytotoxicity and affect DNA replication. **A.** About 2×10^3 of H1299, HeLa, BJ1, or IMR90 cells were seeded in 96-well plates and incubated at 37°C for 24 h. Cells were then washed with PBS, recultured in fresh medium, and incubated with varying amounts of BMVC for another 48 h. The level of cell growth was also determined using MTT assay. The values are obtained from six experiments using the values without drug treatment as 100%. **B.** About 2×10^5 of H1299 cells were seeded in six-well plates and incubated at 37°C for 24 h. Nocodazole at 0.1 μg/mL was added to the cultures and incubated for another 13 h to synchronize cells in M phase. Cells were then washed and subsequently released to cell cycle in the presence or absence of 0.5 μmol/L BMVC. Cells were harvested at indicated time points, stained with 50 μg/mL propidium iodide, and subjected to fluorescence-activated cell sorting analysis. The percentages of S-phase cells were plotted.

concentrations of BMVC >3 μmol/L. The inhibition of BMVC to Taq DNA polymerase was estimated with an IC_{50} value at ~2.5 μmol/L. Thus, although BMVC also affected the PCRs, a higher concentration of BMVC is required. Together, we showed that BMVC is a potent G-quadruplex stabilizer and it selectively inhibits telomerase through direct inhibition of the enzyme activity.

Cellular Effects of BMVC on Viability and Proliferation of Cells

The cellular uptake of BMVC by both cancer and normal cells was first evaluated. By taking the advantage of the BMVC fluorescent property, the level of cellular uptake could be determined readily by a fluorescence microscope. We found that BMVCs were detected in ~70% of the human H1299 cancer cells within 40 min. In contrast, it took over 300 min for the same amount of the normal human IMR90 cells to uptake BMVC, indicating that the uptake of BMVC into cancer cells is more efficient than that of normal cells (data not shown). Short-term cell viability assays were done on human H1299 and HeLa cancer cell lines as well as human normal fibroblasts BJ1 and IMR90. Survival of these cells after incubation with BMVC for 48 h was measured. We found that BMVC did not cause severe cell toxicities at the doses <10 μmol/L (Fig. 2A). No obvious preferential killing toward either cancer or normal cells was observed. Because drug concentration at 0.5 μmol/L of BMVC is sufficient to abolish telomerase activity while causing almost negligible cytotoxicity to cells, we have selected this concentration for further cellular analysis.

In addition to its high affinity binding toward G-quadruplex DNA, BMVC also binds to duplex DNA with relatively low affinity (26). To determine if duplex DNA-binding activity of BMVC affects DNA replication, the progression of S phase was evaluated. H1299 cancer cells were first synchronized in G_2-M phase by nocodazole and then released to determine the progression of cell cycle using fluorescence-activated cell sorting (Fig. 2B). Under this assay condition, our results indicated that 0.5 μmol/L BMVC did not seem to affect the progression of H1299 cells through S phase as the timing and percentage of S-phase cells were similar in both control and BMVC-treated cells.

BMVC-Induced Accelerated Senescence in Cancer Cells

The cellular phenotypes were also analyzed after long-term treatments of cells with nontoxic level of BMVC at 0.5 μmol/L. We found that the lung cancer H1299 cells stopped proliferation after ~10 days, around six population doublings on incubating with BMVC (Fig. 3A). The long-term BMVC-treated H1299 cells showed distinctive morphologic features associated with senescent normal cells. The late passage of 0.5 μmol/L BMVC-treated cells became enlarged, having irregular cell shapes and more distinct nuclei (data not shown). These cells also showed reduction of bromodeoxyuridine (BrdUrd) incorporation and induction of senescence-associated β-galactosidase (SA-β-Gal; Fig. 3B and C). The results clearly indicated that BMVC induced senescence program in cancer cells. The cellular DNA contents of BMVC-treated cells were also analyzed by flow cytometry. The results showed that the treatment using

0.5 μmol/L of BMVC induced a decrease in the percentage of G_0-G_1–phase cells and a slight increase in the percentage of S-phase cells (Fig. 3D). Because BMVC did not affect cell cycle progression in our previous experiments (Fig. 2B), the mechanism of how BMVC increased S-phase population is unclear to us. Interestingly, the percentage of sub-G_1–phase cells was markedly increased after 18 days of BMVC treatments (Fig. 3D). Indeed, the fractions of apoptotic cells analyzed by terminal deoxynucleotidyl transferase–mediated dUTP nick end labeling (TUNEL) assays were increased from ~5% in the early stage of BMVC treatments to ~25% after long treatments of the compound (Fig. 3D). The results indicated that the cancer cells treated with BMVC lead to ceasing of cell growth and eventually cell death through apoptosis.

Similar results were observed for oral cancer CA9-22 cells that they stopped proliferation after BMVC treatments (data not shown). Thus, our results showed that BMVC induced a delayed cellular effect that stopped the proliferation of cells. The long-term cellular effect of BMVC was also evaluated using human normal fibroblasts. On incubating with 0.5 μmol/L BMVC, the normal BJ1 fibroblasts stopped proliferation after around 21 to 24 days (Fig. 4A). Thus, long-term treatments of BMVC also affected the proliferation activity of normal cells, although a long lag period is required for cells to stop proliferating. Further analysis of these long-term treated BJ1 cells indicated that they also entered senescence similar to that in cancer cells (Fig. 4B and C). Because BMVC did not cause acute toxic effects to normal fibroblasts and took a long lag period to affect normal cell proliferation, the later analyses were focused on cancer cells.

The effect of BMVC on telomere length was next evaluated. The genomic DNAs were prepared from H1299 cells treated with 0.5 μmol/L BMVC at different time intervals and then analyzed by Southern hybridization using radioactive telomeric DNA as the probe. We estimated that BMVC-treated cells caused telomere shortening at a rate of ~420 bp per population doubling (Fig. 5A), a rate that is much faster than the rate of around 50 to 200 bp per population doubling in human normal cells (33). Thus, BMVC seems to accelerate telomere shortening in H1299 cancer cells. Interestingly, although long-term treatments of BMVC caused similar antiproliferation effects on normal BJ1 cells, the telomeres of these cells did not

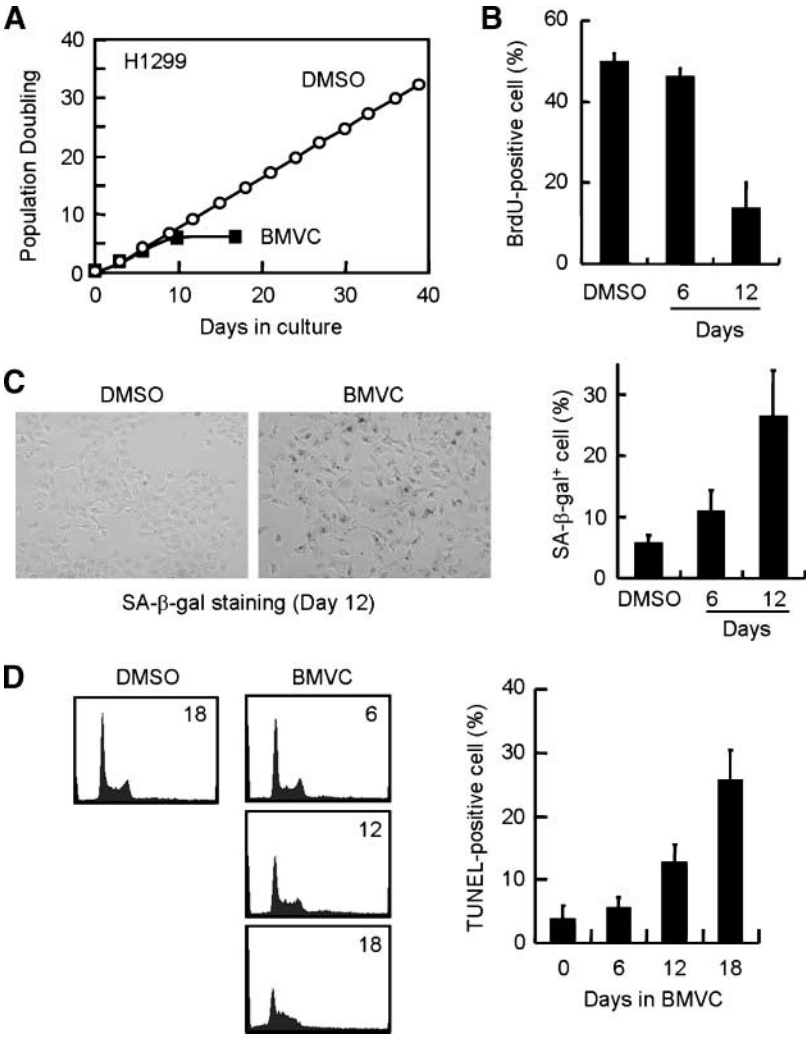

FIGURE 3. Senescent phenotype of BMVC-treated cancer cells. **A.** Delayed antiproliferation activity of BMVC. H1299 cells were treated with 0.5 μmol/L of BMVC. The numbers of cells were counted during the passages and the population doubling numbers were determined. Results were obtained from the average of three independent experiments. **B.** Suppression of BrdUrd incorporation in BMVC-treated cancer cells. H1299 cells were treated with 0.5 μmol/L of BMVC and labeled with BrdUrd. After labeling, the cells were fixed and stained with anti-BrdUrd antibody. The percentage of BrdUrd-positive cells was presented. **C.** Detection of SA-β-Gal in BMVC-treated H1299 cells. H1299 cells were treated without (DMSO) or with 0.5 μmol/L of BMVC and subjected to staining for SA-β-Gal. Photographs of the 5-bromo-4-chloro-3-indolyl-β-D-galactopyranoside–stained cells are shown. The levels of SA-β-Gal–positive cells were also measured. **D.** Induction of apoptosis in long-term BMVC-treated H1299 cells. Cell cycle effects of BMVC-treated H1299 cells. Left, flow cytometry analysis of BMVC-treated H1299 cells was conducted after 6, 12, or 18 d of treatments; right, TUNEL analyses were conducted on 0, 6, 12, or 18 d of BMVC-treated cells and the percentages of TUNEL-positive cells were calculated.

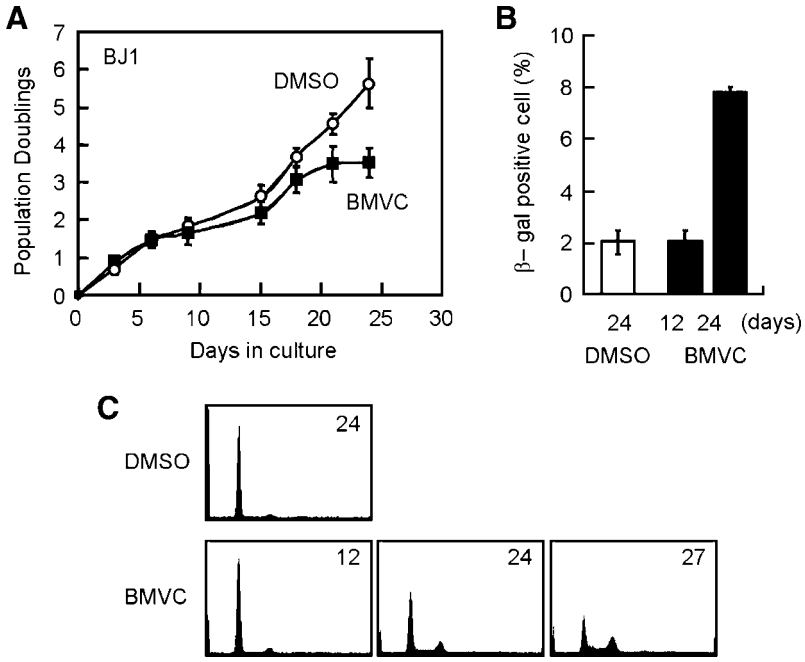

FIGURE 4. Senescent phenotype of BMVC-treated normal cells. **A.** Delayed antiproliferation activity of BMVC. BJ1 cells were treated with 0.5 μmol/L of BMVC. The numbers of cells were counted during the passages and the population doubling numbers were determined. Results were obtained from the average of three independent experiments. **B.** Detection of SA-β-Gal in BMVC-treated BJ1 cells. BJ1 cells were treated without (DMSO) or with 0.5 μmol/L of BMVC and subjected to staining for SA-β-Gal. The levels of SA-β-Gal–positive cells were also measured. **C.** Cell cycle effects of BMVC-treated BJ1 cells. Flow cytometry analysis of BMVC-treated BJ1 cells was conducted after 12, 24, or 27 d of treatments.

seem to be shortened faster than that of the untreated cells (data not shown). Telomere shortening eventually leads to telomere uncapping that in turn induces DNA damage signals for cell cycle arrest (34). We further analyzed the effect of BMVC on induction of DNA damage signals using the nucleus accumulation of γ-H2AX as the criteria. It is apparent that BMVC did not induce significant γ-H2AX accumulation for up to 6 days of treatment (Fig. 5B). The γ-H2AX signals became apparent after treating the cells for 9 days. At day 12, up to 40% of the BMVC-treated cells showed γ-H2AX staining (Fig. 5C). The results indicated that the DNA damage signals were induced in long-term BMVC-treated cancer cells. To test if the DNA damage foci were due to telomere uncapping, the localization of the DNA damage foci and telomeres was revealed by costaining of γ-H2AX and telomere binding protein TRF2 using confocal microscope. Results in Fig. 5D clearly indicated that these two proteins were colocalized, indicating that long-term treatments of BMVC caused telomere uncapping.

BMVC-Treated Cancer Cells Lost Tumorigenic Properties In vitro

Immortality is a key property for most of the cancer cells. To further determine if BMVC affects other properties of cancer cells, we evaluated the colony-forming, anchorage-independent growth, and migration properties of cancer cells treated by BMVC. Cancer cells tend to decrease density-dependent inhibition of growth and pile up in culture rather than stop growing when they come into contact. This property can be determined through seeding diluted cells in culture plates and observing the colony-forming ability of individual cells. The H1299 cells were pretreated with varying amounts of BMVC for 6 days and the colony-forming abilities of treated cells without further BMVC treatments were analyzed. It is apparent that 0.5 μmol/L of BMVC treatments completely abolished colony formation in our assays, indicating that BMVC affected the colony-forming property of cancer cells (Fig. 6A, *Pre-treatment*). To rule out the possibility that cancer cells failed to form colony owing to the loss of cell proliferation, the cells were seeded and then cotreated with BMVC during the colony-forming period. Similar results were observed, although greater amounts of BMVC were required to achieve the same level of inhibition (Fig. 6A, *Co-treatment*). Because we have shown that the proliferating properties of cancer cells were not affected in the first 7 days (Fig. 3A), equivalent to the time required for colonies to form, these results indicated that H1299 cells lost colony-forming ability after BMVC treatments. Moreover, because the cancer cells have not entered senescence during the assays, our results further suggest that BMVC affected cancer cells in a senescence-independent manner.

Anchorage-independent growth of cancer cells on soft agar is considered as an *in vitro* assay for tumorigenic potential of cancer cells. We next evaluated the effects of BMVC on anchorage-independent growth of cancer cells. The soft agar assays were conducted using H1299 cells that were either being pretreated with varying amounts of BMVC for 6 days or cotreated with BMVC during the colony-forming period. As shown in Fig. 6B, the numbers of colonies were greatly reduced for cancer cells that were either pretreated or cotreated with BMVC. Thus, BMVC seemed to suppress the anchorage-independent growth of cancer cells.

Migration of cancer cells is necessary for the initiation of the metastasis cascade. The effects on the migration of H1299 cells were evaluated. Here, the cells were seeded on plates, and when cells grew to near confluent, a scratch was made on the plate to generate a cell-free zone. The migration of cells into the cell-free zone was then measured at different time intervals to calculate the migration rate. The experiments were conducted under low serum condition (1%) so that no further cell divisions

were detected during the observation period. The results clearly showed that the migration rates of H1299 cells either cotreated or pretreated with BMVC were reduced (Fig. 6C). Thus, BMVC also affects the migration of cancer cells.

BMVC Delayed Tumorigenic Potential of Cancer Cells In vivo

This tumor xenograft model was also used to examine the inhibition of tumor formation by BMVC. The toxicity of BMVC on mice was first evaluated. We found that nude mice ($n = 4$) injected i.p. with 0.2 or 1 mg/kg of BMVC every 3 days showed no sign of acute toxicity and no change in body weight for up to 140 days. However, mice showed body weight loss and sickness after injection of 5 mg/kg BMVC for ~20 days, indicating BMVC toxicity at this concentration (data not shown). Thus, we injected 2×10^6 H1299 cells s.c. to nude mice ($n = 6$) until tumors grew to around 50 to 100 mm^3 and then evaluated the effect of BMVC on tumor growth at the dose of 1 mg/kg. During the experimental periods, the body weights of BMVC-treated mice were similar to those of the control mice (Fig. 7A). On the other hand, the growth rates of tumors in BMVC-treated animals were significantly slower than that of control animals (Fig. 7B). The results indicated that BMVC treatment is sufficient to inhibit the progression of tumor growth. We next tested if the BMVC tumor cells entered apoptosis using TUNEL assays. The results shown in Fig. 7C indicated that tumor cells of the BMVC-treated mice were indeed entering apoptosis. The cryosections of tumors were also observed directly under fluorescence microscope to determine the uptake of BMVC by tumor cells. Results shown in Fig. 7D indicated that BMVC fluorescences were detected in the nucleus of most tumor cells taken from BMVC-treated mice. Thus, the growth of tumor in BMVC-treated mice was not due to failed entry of BMVC into tumor cells.

Discussion

In general, inhibitors for telomerase enzyme do not induce cytotoxicity immediately after treatment (8, 35). Complete inhibition of cancer cell proliferation will require continued cell division until their telomeres reach a critical short length. For example, HeLa cells treated with oligonucleotides targeting telomerase RNA showed senescence phenotype after ~20 cell divisions (8). This lag in therapeutic response allows cancer cells to grow for a period of time. Here, we show that BMVC, a novel carbazole derivative, inhibits telomerase activity and induced senescence in drug-treated cells, consistent with the predicted properties of a telomerase inhibitor. Moreover, there are several unique features presented by the BMVC-treated cells. First, in contrast to the telomere shortening rates of around 50 to 200 nucleotides of normal human cells (10, 11),

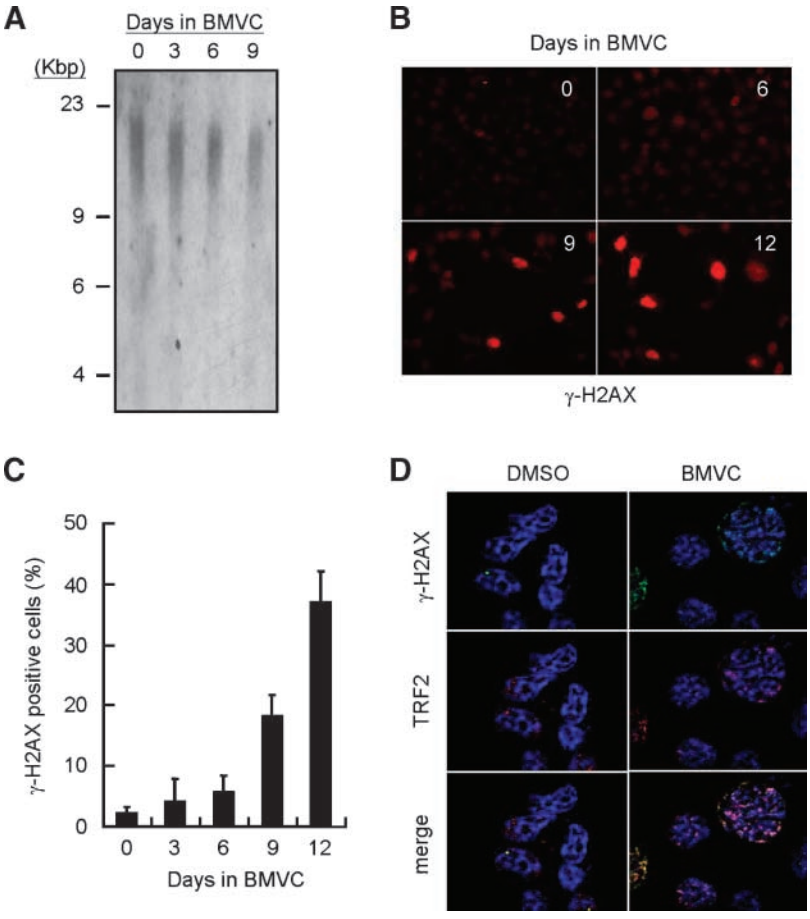

FIGURE 5. Induction of telomere uncapping by BMVC. **A.** Effects of BMVC on telomere length. H1299 cells were treated with BMVC and total genomic DNA was prepared and analyzed for telomere length by Southern blotting using telomeric DNA as the probe. **B.** Induction of DNA damage foci in BMVC-treated cells. H1299 cells were treated with 0.5 μmol/L of BMVC for 3, 6, 9, or 12 d and stained with antibody against γ-H2AX. Staining of DNA by Hoechst 33258 was used to locate the positions of nuclei. **C.** The percentages of γ-H2AX–positive cells were quantified. **D.** Telomere uncapping observed in BMVC-treated H1299 cells. H1299 cells were treated with 0.5 μmol/L of BMVC for 12 d and stained with antibodies against γ-H2AX and TRF2.

the telomeres of BMVC-treated H1299 cells shortened at a rate of ~420 nucleotides per round of cell division. Accordingly, the treated cells showed a short lag period before entering senescence. Second, the BMVC-treated cells lost several of tumor properties, including colony-forming, anchorage-independent growth, and migration activities. It is also to our surprise that BMVC is capable of inhibiting tumor growth in nude mice. Although the mechanism of how BMVCs affect the tumorigenic potential of cancer cells is still unclear, BMVC represents a novel type of telomerase inhibitors that has multiple effects to cancer cells and has the potential for future anticancer drug developments.

The multiple effects of BMVC cannot be simply explained by telomerase inhibition or telomere shortening. Because BMVC has a G-quadruplex stabilizing activity, it is possible that the target for BMVC is not only limited to telomeres. Chromosome regions rich in G residues that have the potential to be induced to form G-quadruplex structure could also be the target of BMVC. Thus, in addition to its effects on telomeres, BMVC also affects cancer cells in a telomere-independent manner. Indeed, a bioinformatic survey of human chromosome for putative G-quadruplex–forming sequences has identified over 375,000 sequences (36, 37). It was also found that these putative G-quadruplex–forming sequences seem to be preferentially located in proto-oncogenes (38). Although it remains to be tested for the biological relevance of these sequences, several of these sequences are indeed capable of forming G-quadruplex structures. For example, the G-rich region within the promoter sequences of *c-myc, VEGF, c-kit, BCL2*, and *KRAS* proto-oncogenes was capable of forming G-quadruplex structures (39-43). Moreover, stabilization of G-quadruplex structures by small-molecule compounds represses the expression of *c-myc* (39). Thus, these DNA sequences of tumorigenesis-related genes might be the targets for BMVC that inhibits the tumorigenic potential in cancer cells. Consistent with this notion, here we observed the inhibition of normal cell proliferation after long-term BMVC treatments, although a long lag period is required. Similarly, a recent report also indicated that a group of selective G-quadruplex stabilizers was capable of limiting the growth of SAOS-2 cell, a cell line where its telomeres were maintained by alternative lengthening of telomere pathway (44). Thus, it is likely that a portion of the cellular effects of BMVC is through its G-quadruplex stabilizing activity in a telomere-independent manner. Alternatively, it was shown that telomerase could have a role on tumor progression in a telomere-independent manner (45, 46). Immortal cells maintained by alternative mechanism of telomere maintenance or telomerase behaved differently in oncogene-induced transformation or tumor metastasis. Thus, although the molecular mechanism of how BMVC rendered its anticancer effects is still unclear, it is likely that telomerase inhibition or telomere shortening is not the only factor for how BMVC inhibited tumor formation and progression.

In addition to BMVC, there were many telomerase inhibitors that have been identified based on G-quadruplex stabilizing activity (20-24). The effects of BMVC on cancer cells are somewhat different from that by other G-quadruplex ligands. For example, 2,6-pyridine-dicarboxamide derivatives and 3,6,9-trisubstituted acridine compounds caused accelerated senescence in cancer cells without significant telomere shortening in these drug-treated cells (44, 47). It was also shown that telomestatin induced uncapping of telomeres by causing telomere binding protein TRF2 or POT1 to dissociate from

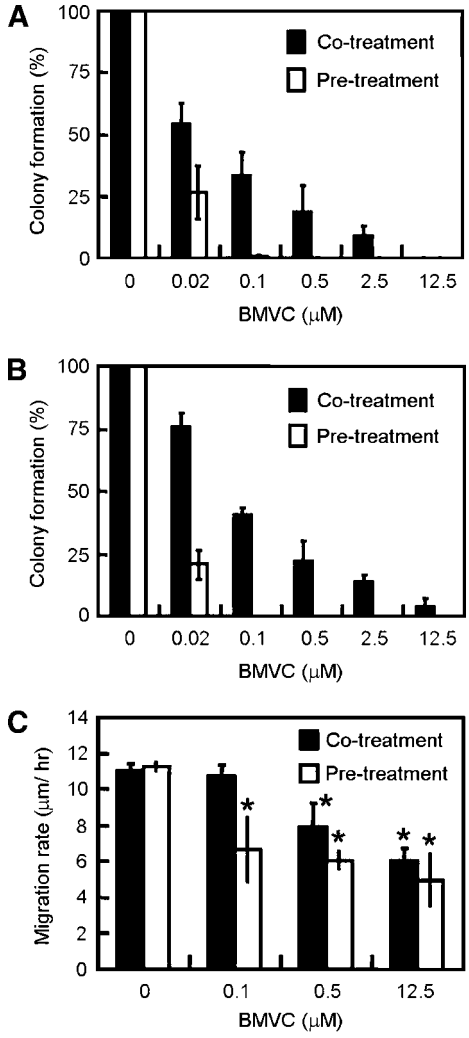

FIGURE 6. *In vitro* anticancer activities of BMVC. **A.** Colony-forming ability of cancer cells is suppressed by BMVC. For pretreatment experiments, H1299 cells were treated with varying amounts of BMVC for 6 d and seeded at a density of 1,000 per well. The cells were then grown without further BMVC treatments at 37°C for another 7 d. For cotreatment experiments, H1299 cells were seeded and grown in the presence of varying amounts of BMVC for 7 d. Colonies were stained by MTT and quantified. Quantification results were obtained from the average of three independent experiments. The number of colonies without BMVC treatments was taken as 100%. **B.** Anchorage-independent growth of cancer cells is suppressed by BMVC. The experiments were conducted similar to that described in **A**. H1299 cells were seeded at a density of 2,000 per well on 0.2% agar-coated plates. The cells were then grown at 37°C for another 14 d. Colonies were stained by MTT and quantified. **C.** The migration ability of cancer cells is suppressed by BMVC. H1299 cells were treated with 0.1, 0.5, or 12.5 μmol/L of BMVC for 6 d (*Pre-treatment*). Around 20,000 cells were seeded on coverslips and incubated overnight. The coverslips were then scratched with a yellow tip to generate a cell-free zone. Indicated amounts of BMVC were added to the cells (*Co-treatment*). Migration of cells toward the cell-free zone was then monitored every 6 h and the migration rates were determined. The migration rates were plotted. Columns, mean of four independent experiments; bars, SD. Statistical analyses were conducted using Student's *t* tests. *, significantly different from no BMVC control ($P < 0.05$).

telomeres (48). Here, we show that BMVC induced accelerated telomere shortening and inhibited tumorigenic potential in H1299 cells. Thus, it is apparent that these inhibitors affect telomere differently. The specificity and affinity of these compounds toward G-quadruplex DNA might contribute to their different effects on telomeres. In addition, the "off-target" effects of these compounds could also contribute to the variations of cellular effects. Thus, although telomeres are the primary molecular target for BMVC, that it causes accelerated telomere shortening and telomere uncapping, other mechanism might also contribute to its cellular function. Although the mechanism of how BMVCs affect accelerated telomere shortening and tumorigenesis remained to be elucidated, nevertheless, BMVC represents a novel group of G-quadruplex stabilizers that has the potential to be further developed to be anticancer drugs.

Materials and Methods

Chemistry

Carbazole and 3,6-dibromocarbazole were purchased from Aldrich and used without further purification. The synthesis of BMVC has been described previously (49).

Tm *Measurement*

The *Tm* was measured by monitoring the circular dichroism maximum at 295 nm on a Jasco J-715 spectropolarimeter with ramping the temperature from 5°C to 90°C at a rate of 0.8°C/min. Oligonucleotide $d(TTAGGG)_4$ was purchased from Applied Biosystems. Solutions of 10 mmol/L Tris-HCl (pH 7.5) and 150 mmol/L NaCl mixed with DNA were heated to 90°C for 2 min, cooled slowly to room temperature, and then stored for 42 h at 4°C before use. The molar concentration of DNA was determined by monitoring the 260 nm absorbance. The $d(T_2AG_3)_4$ DNA forms a G-quadruplex structure at room temperature as indicated by the 295 nm positive circular dichroism band detected at 25°C.

Telomerase Activity Assay

The ability of agents to inhibit telomerase in a cell-free assay was assessed with a TRAP assay (31). A modified TRAP-G4 was also used for G-quadruplex–induced telomerase activity assay (30). Telomerase-extended products were resolved by 10% PAGE and visualized by SYBER Green I staining of the gel. As a source for telomerase, total cell lysates derived from lung cancer cell line H1299 cells were used. Protein concentration of the lysates was determined by means of a Bio-Rad assay kit and with bovine serum albumin as standards.

Cell Viability Assay

Cells were grown in 96-well plates (~2,000 per well) in a 5% CO_2 incubator at 37°C. To examine the short-term cytotoxic effect, cells were then incubated with different concentrations of BMVC for 72 h. The cytotoxicity was determined by 3-(4,5-dimethylthiazol-2-yl)-2,5-diphenyltetrazolium bromide (MTT) and analyzed spectrophotometrically at the absorbance of 570 nm.

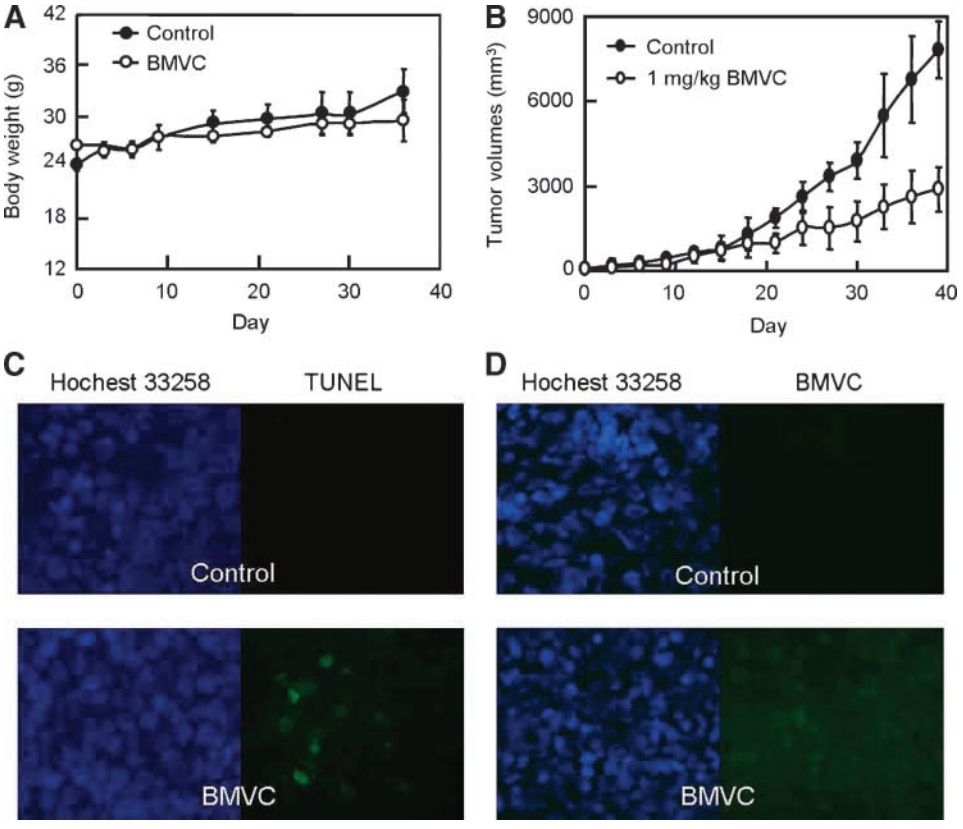

FIGURE 7. BMVC suppresses tumor formation. Nude mice ($n = 6$) were each injected with 2×10^6 H1299 cells. BMVC at 1 mg/kg was injected every 3 d. The body weight (**A**) and tumor size (**B**) were then measured. The cryosections of tumors stained with TUNEL (**C**) or visualized directly under fluorescence microscope (**D**) were also presented.

Population Doubling Study

Cells were treated with 0.5 μmol/L BMVC or DMSO (drug vehicle control) and grown in T25 tissue culture flasks at 3×10^5 per flask for 3 or 4 d and then trypsinized and counted. Each time, 3×10^5 cells were replaced in the new culture flask with fresh BMVC or an equivalent volume of DMSO. The experiments were continued until there were fewer than 3×10^5 cells available for reseeding. The results were obtained from at least three independent experiments.

SA-β-Gal Staining

Detection of SA-β-Gal followed the standard protocol (50). Briefly, cells were washed in PBS, fixed in 2% formadehyde/0.2% glutaldehyde (or 3% formaldehyde), and incubated at 37°C with 1 mg/mL of fresh-prepared SA-β-Gal stain solution. Staining was evident in 2 to 4 h and maximal in 24 to 48 h.

BrdUrd Incorporation

The BMVC-treated H1299 cells were incubated with 100 μmol/L BrdUrd for 2 h. The cells were then washed with PBS, fixed by paraformaldehyde, and stained with monoclonal antibody against BrdUrd (BU-33; Sigma). Horseradish peroxidase–conjugated secondary antibody against mouse IgG was added to the cells and visualized by 3,3′-diaminobenzidine tetrahydrochloride stain. Hematoxylin staining was used as counterstains.

Telomere Length Determination

Cells were treated with 0.5 μmol/L BMVC or DMSO (drug vehicle control) for 3, 6, or 9 d and total genomic DNA was prepared using the extraction kit purchased from BD Biosciences Clontech. To determine the telomere length, genomic DNA was digested with *Hin*fI and *Rsa*I and separated by 1% agarose gel electrophoresis. After electrophoresis, the DNA was transferred onto a Hybond N^+ (Amersham Biosciences Ltd.) membrane and hybridized with ^{32}P-labeled ~800 bp $(TTAGGG)_n$ fragments. Telomeric smears were visualized and quantified with a PhosphorImager (Molecular Dynamics).

Immunofluorescence Analysis

H1299 cells were treated with BMVC, fixed, and incubated with anti-γ-H2AX antibody (JBW301; Upstate). Visualization of γ-H2AX was achieved by addition of rhodamine-conjugated anti-mouse IgG (Rhodamine Red-X conjugated; Jackson) and observed under fluorescence microscopy (Olympus BX50). Confocal analysis was conducted using anti-γ-H2AX antibody (ab2893; Abcam) and anti-TRF2 antibody (4A794-15; Imgenex). Visualization of γ-H2AX and TRF2 was achieved by addition of fluorescein FITC-conjugated anti-rabbit IgG (FITC conjugated; Jackson) and rhodamine-conjugated anti-mouse IgG (Rhodamine Red-X conjugated) and then observed under laser confocal microscopy (Olympus FV1000).

Flow Cytometry Assays

Cells growing on 6-cm culture dishes were treated with 0.5 μmol/L of BMVC for different durations in a 5% CO_2 incubator at 37°C. The cells were then collected by trypsinization, washed with PBS, fixed with 70% alcohol, and stained with propidium iodide at the concentration of 1.5 μg/mL. Samples were analyzed by flow cytometry (FACSCalibur and CellQuest software, BD Biosciences).

Colony-Forming and Anchorage-Independent Growth Assays

H1299 cells were treated with varying amounts of BMVC for 6 d and seeded at a density of 1,000 per well onto six-well plates. The cells were then grown without further BMVC treatments at 37°C for another 7 d. In the cotreatment experiments, the cells were grown in the presence of varying amounts of BMVC without pretreatment with BMVC. Visualization of colonies formed was achieved by staining the cells with 1 mg/mL MTT in serum-free condition for 4 h. The photograph was taken and the number of colonies was measured. For anchorage-independent growth assays, the ability of cells grown on soft agar was used as the criteria. Similarly, ~2,000 BMVC-treated H1299 cells were mixed with 0.2% agar and seeded onto culture plates that were precoated with 0.5% agar. The cells were grown for another 2 wk before MTT staining and quantifications.

Cell Migration Assay

H1299 cells were treated with varying amounts of BMVC (pretreatment) or without BMVC (cotreatment) for 6 d. Around 20,000 cells were seeded on coverslips and incubated overnight. The coverslips were then scratched with a yellow tip to generate a cell-free zone. Varying concentrations of BMVC were then added to the cells in cotreatment experiments. Migration of cells toward the cell-free zone was monitored every 6 h and the migration rates were determined.

TUNEL Assays

H1299 cells were fixed with 4% formaldehyde after BMVC treatment and TUNEL assays were conducted using commercial kit (TdT-FragEL DNA Fragmentation Detection kit, Calbiochem). Incorporation of BrdUrd into the fragmenting nuclear DNA was detected by horseradish peroxidase–conjugated anti-BrdUrd antibody and visualized by 3,3′-diaminobenzidine tetrahydrochloride stain. Methyl green staining was used as counterstains. For tissue sections, mice bearing tumors were sacrificed after BMVC treatment for 42 d. An *in situ* cell death detection kit (Roche) was used to detect apoptosis on cryostat sections. The fluorescein-dUTP was used to detect DNA fragmentations. Visualization of fluorescein incorporation was achieved using a fluorescence microscope.

Animal Studies

Around 2×10^6 of lung cancer H1299 cells were injected s.c. into BALB/cAnN.Cg-Foxn1^{nu}/CrlNarl mice (National Laboratory Animal Center, Taipei, Taiwan, Republic of China). BMVC at concentration of 1 mg/kg was injected i.p. every 3 d after the tumor grew to around 50 to 100 mm^3. Growth of the tumors was recorded by caliper measurements determining length (L) and width (W) of the s.c. tumor mass. The tumor volumes were estimated as $LW^2/2$.

Acknowledgments

We thank members of the Institute of Biopharmaceutical Science for their help and support and Drs. Ting-Fen Tsai and Chun-Ming Chen for their assistance in animal analysis.

References

1. Blasco MA. Telomeres and human disease: ageing, cancer and beyond. Nat Rev Genet 2005;6:611–22.

2. Cech TR. Beginning to understand the end of the chromosome. Cell 2004;116: 273–9.

3. Ferreira MG, Miller KM, Cooper JP. Indecent exposure: when telomeres become uncapped. Mol Cell 2004;13:7–16.

4. Collins K, Mitchell JR. Telomerase in the human organism. Oncogene 2002; 21:564–79.

5. Shay JW, Bacchetti S. A survey of telomerase activity in human cancer. Eur J Cancer 1997;33:787–91.

6. Shay JW, Wright WE. Telomerase therapeutics for cancer: challenges and new directions. Nat Rev Drug Discov 2006;5:577–84.

7. Shay JW, Wright WE. Telomerase: a target for cancer therapeutics. Cancer Cell 2002;2:257–65.

8. Feng J, Funk WD, Wang SS, et al. The RNA component of human telomerase. Science 1995;269:1236–41.

9. Neidle S, Parkinson G. Telomere maintenance as a target for anticancer drug discovery. Nat Rev Drug Discov 2002;1:383–93.

10. Harley CB, Futcher AB, Greider CW. Telomeres shorten during ageing of human fibroblasts. Nature 1990;345:458–60.

11. Canela A, Vera E, Klatt P, Blasco MA. High-throughput telomere length quantification by FISH and its application to human population studies. Proc Natl Acad Sci U S A 2007;104:5300–5.

12. Ludwig A, Saretzki G, Holm PS, et al. Ribozyme cleavage of telomerase mRNA sensitizes breast epithelial cells to inhibitors of topoisomerase. Cancer Res 2001;61:3053–61.

13. Chen Z, Koeneman KS, Corey DR. Consequences of telomerase inhibition and combination treatments for the proliferation of cancer cells. Cancer Res 2003; 63:5917–25.

14. Biroccio A, Gabellini C, Amodei S, et al. Telomere dysfunction increases cisplatin and ecteinascidin-743 sensitivity of melanoma cells. Mol Pharmacol 2003;63:632–8.

15. Tauchi T, Nakajima A, Sashida G, et al. Inhibition of human telomerase enhances the effect of the tyrosine kinase inhibitor, imatinib, in BCR-ABL-positive leukemia cells. Clin Cancer Res 2002;8:3341–7.

16. Sen D, Gilbert W. Novel DNA superstructures formed by telomere-like oligomers. Biochemistry 1992;31:65–70.

17. Zahler AM, Williamson JR, Cech TR, Prescott DM. Inhibition of telomerase by G-quartet DNA structures. Nature 1991;350:718–20.

18. Mergny J-L, Helene C. G-quadruplex DNA: a target for drug design. Nat Med 1998;4:1366–7.

19. Han H, Hurley LH. G-quadruplex DNA: a potential target for anticancer drug design. Trends Pharmacol Sci 2000;21:136–42.

20. Sun D, Thompson B, Cathers BE, et al. Inhibition of human telomerase by a G-quadruplex-interactive compound. J Med Chem 1997;40:2113–28.

21. Read M, Harrison RJ, Romagnoli B, et al. Structure-based design of selective and potent G-quadruplex-mediated telomerase inhibitors. Proc Natl Acad Sci U S A 2001;98:4844–9.

22. Heald RA, Modi C, Cookson JC, et al. Antitumor polycyclic acridines. 8. Synthesis and telomerase-inhibitory activity of methylated pentacyclic acridinium salts. J Med Chem 2002;45:590–7.

23. Gowan SM, Heald R, Stevens MF, Kelland LR. Potent inhibition of telomerase by small-molecule pentacyclic acridines capable of interacting with G-quadruplexes. Mol Pharmacol 2001;60:981–8.

24. Wheelhouse RT, Sun D, Han H, Han FX, Hurley LH. Cationic porphyrins as telomerase inhibitors: the interaction of tetra-(*N*-methyl-4-pyridyl)porphine with quadruplex DNA. J Am Chem Soc 1998;120:3261–2.

25. Chang CC, Kuo IC, Lin JJ, et al. A novel carbazole derivative, BMVC: a potential antitumor agent and fluorescence marker of cancer cells. Chem Biodivers 2004;1:1377–84.

26. Chang CC, Kuo IC, Ling IF, et al. Detection of quadruplex DNA structures in human telomeres by a fluorescent carbazole derivative. Anal Chem 2004;76: 4490–4.

27. Jin R, Gaffney BL, Wang C, Jones RA, Breslauer KJ. Thermodynamics and structure of a DNA tetraplex: a spectroscopic and calorimetric study of the tetramolecular complexes of d(TG3T) and d(TG3T2G3T). Proc Natl Acad Sci U S A 1992;89:8832–6.

28. Scaria PV, Shire SJ, Shafer RH. Quadruplex structure of d(G3T4G3) stabilized by K^+ or Na^+ is an asymmetric hairpin dimer. Proc Natl Acad Sci U S A 1992;89:10336–40.

29. Chang CC, Chien CW, Lin YH, Kang CC, Chang TC. Investigation of spectral conversion of d(TTAGGG)4 and d(TTAGGG)13 upon potassium titration by a G-quadruplex recognizer BMVC molecule. Nucleic Acids Res 2007;35:2846–60.

30. Gomez D, Mergny J-L, Riou JF. Detection of telomerase inhibitors based on G-quadruplex ligands by a modified telomeric repeat amplification protocol assay. Cancer Res 2002;62:3365–8.

31. Kim NW, Piatyszek MA, Prowse KR, et al. Specific association of human telomerase activity with immortal cells and cancer. Science 1994;266:2011–5.

32. De Cian A, Cristofari G, Reichenbach P, et al. Reevaluation of telomerase inhibition by quadruplex ligands and their mechanisms of action. Proc Natl Acad Sci U S A 2007;104:17347–52.

33. Bond JA, Blaydes JP, Rowson J, et al. Mutant p53 rescues human diploid cells from senescence without inhibiting the induction of SDI1/WAF1. Cancer Res 1995;55:2404–9.

34. Takai H, Smogorzewska A, de Lange T. DNA damage foci at dysfunctional telomeres. Curr Biol 2003;13:1549–56.

35. Damm K, Hemmann U, Garin-Chesa P, et al. A highly selective telomerase inhibitor limiting human cancer cell proliferation. EMBO J 2001;20:6958–68.

36. Huppert J, Balasubramanian S. Prevalence of quadruplexes in the human genome. Nucleic Acids Res 2005;33:2908–16.

37. Todd AK, Johnston M, Neidle S. Highly prevalent putative quadruplex sequence motifs in human DNA. Nucleic Acids Res 2005;33:2901–7.

38. Eddy J, Maizels N. Gene function correlates with potential for G4 DNA formation in the human genome. Nucleic Acids Res 2006;34:3887–96.

39. Siddiqui-Jain A, Grand CL, Bearss DJ, Hurley LH. Direct evidence for a G-quadruplex in a promoter region and its targeting with a small molecule to repress c-MYC transcription. Proc Natl Acad Sci U S A 2004;99:11593–8.

40. Rankin S, Reszka AP, Huppert J, et al. Putative DNA quadruplex formation within the human c-kit oncogene. J Am Chem Soc 2005;127:10584–9.

41. Sun D, Guo K, Rusche JJ, Hurley LH. Facilitation of a structural transition in the polypurine/polypyrimidine tract within the proximal promoter region of the human VEGF gene by the presence of potassium and G-quadruplex-interactive agents. Nucleic Acids Res 2005;33:6070–80.

42. Dai J, Dexheimer TS, Chen D, et al. An intramolecular G-quadruplex structure with mixed parallel/antiparallel G-strands formed in the human BCL-2 promoter region in solution. J Am Chem Soc 2006;128:1096–8.

43. Cogoi S, Xodo LE. G-quadruplex formation within the promoter of the KRAS proto-oncogene and its effect on transcription. Nucleic Acids Res 2006;34: 2536–49.

44. Pennarun G, Granotier C, Gauthier LR, et al. Apoptosis related to telomere instability and cell cycle alterations in human glioma cells treated by new highly selective G-quadruplex ligands. Oncogene 2005;24:2917–28.

45. Stewart SA, Hahn WC, O'Connor BF, et al. Telomerase contributes to tumorigenesis by a telomere length-independent mechanism. Proc Natl Acad Sci U S A 2002;99:12606–11.

46. Chang S, Khoo CM, Naylor ML, Maser RS, DePinho RA. Telomere-based crisis: functional differences between telomerase activation and ALT in tumor progression. Genes Dev 2003;17:88–100.

47. Burger AM, Dai F, Schultes CM, et al. The G-quadruplex-interactive molecule BRACO-19 inhibits tumor growth, consistent with telomere targeting and interference with telomerase function. Cancer Res 2005;65:1489–96.

48. Tahara H, Shin-Ya K, Seimiya H, Yamada H, Tsuruo T, Ide T. G-quadruplex stabilization by telomestatin induces TRF2 protein dissociation from telomeres and anaphase bridge formation accompanied by loss of the 3′ telomeric overhang in cancer cells. Oncogene 2006;25:1955–66.

49. Chang CC, Wu JY, Chang TC. A carbazole derivative synthesis for stabilizing the quadruplex structure. J Chin Chem Soc 2003;50:185–8.

50. Dimri GP, Lee X, Basile G, et al. A biomarker that identifies senescent human cells in culture and in aging skin *in vivo*. Proc Natl Acad Sci U S A 1995; 92:9363–7.